

Demystifying Fractal Analysis of Thin Films: A Reference for Thin Film Deposition Processes



F. M. Mwema , Esther T. Akinlabi , and O. P. Oladijo 

Abstract In this article, a variety of synthetic (or simulated) surfaces of various morphologies of thin films and their fractal analyses are presented. Similar scaling factors have been used to generate the synthetic images in Gwydion™ software. The surfaces are based on the actual morphologies arising from various thin film deposition techniques. Using actual thin films of CdTe deposited by radio-frequency (RF) sputtering technique, we have successfully shown that the fractal analyses on the synthetic surfaces can be used to explain, theoretically, the development and self-affinity of various thin films. Based on this validation, the results of fractal analyses on different morphologies of thin films were generated using different fractal methods in Gwydion software. The methods used here include Minkowski functionals, height-to-height correlation, areal autocorrelation, and power spectral density functions. The article will be a good resource for explaining the fractal behavior and morphology of thin films arising from different deposition methods.

Keywords Correlation · Fractal · Minkowski · Surfaces · Thin films

1 Introduction

During the deposition process of thin films, there are different morphologies of structures formed depending on the deposition type, process parameters, films, and substrate types [1]. Scanning probe microscopy (SPM) techniques such as atomic force microscope (AFM) are used to study the surface morphology of various thin films and coatings [2–5]. The micrographs obtained from the SPM techniques are used to undertake roughness analyses such as statistical [6, 7] and fractal measurements [8–12]. Fractal methods offer a detailed description of lateral roughness [13] and the nature of the surface morphology can be captured [14]. Although fractal

F. M. Mwema (✉) · E. T. Akinlabi · O. P. Oladijo
University of Johannesburg, Johannesburg, South Africa
e-mail: fredrick.mwema@dkut.ac.ke

O. P. Oladijo
Botswana International University of Science and Technology, Palapye, Botswana

© Springer Nature Singapore Pte Ltd. 2021
E. T. Akinlabi et al. (eds.), *Trends in Mechanical and Biomedical Design*,
Lecture Notes in Mechanical Engineering,
https://doi.org/10.1007/978-981-15-4488-0_19

characterization is widely reported in the literature [6, 12, 15–17], very little is reported on the relationship between the fractal measurements and the structure type/morphologies of the films. Therefore, the purpose of this work is to generate fractal profiles (using Minkowski functionals, autocorrelation, height-height correlation, and power spectral density functions) based on theoretical/synthetic surfaces of different morphologies.

2 Methods

Various synthetic morphologies of thin films were produced using scanning probe microscopy (SPM) software Gwydion (Fig. 1). These films depict different structural types that are obtained through various deposition processes such as sputtering and thermal spray. These structures are columnar, ballistic, fibrous, and pile-up structures (Fig. 1) and represent some of the most common morphologies observed in thin films. The process of creating synthetic (simulated) surfaces in Gwydion software are described elsewhere [18, 19]. All the images were single-layer, with a maximum

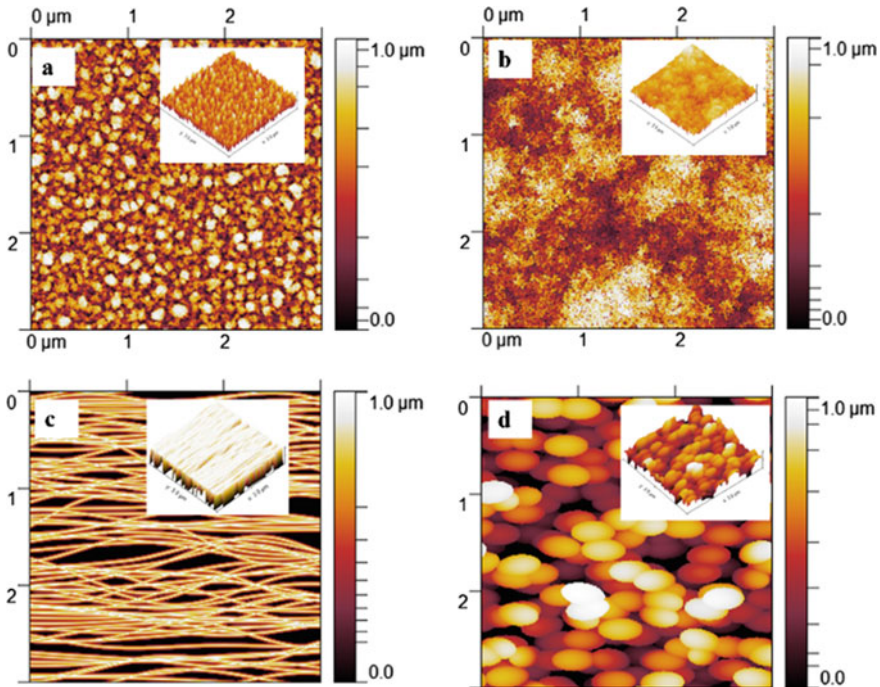


Fig. 1 Illustrating simulated surfaces of thin films consisting of various structural morphologies **a** columnar **b** ballistic **c** fibrous, and **d** pile-up particles. Corresponding 3D images are shown as insets on each image

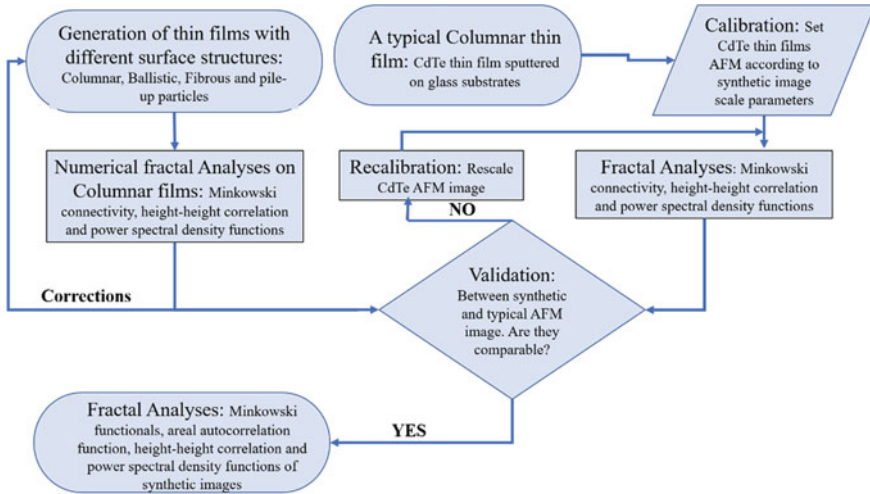


Fig. 2 Flowchart illustrating the image and fractal analyses procedures

height of 1000 nm and a scan area of $3 \times 3 \mu\text{m}^2$. The fractal analyses of the simulated AFM images were undertaken according to the flowchart in Fig. 2. To validate the simulated fractal analyses, fractal values of a typical columnar AFM of CdTe thin films sputtered on glass substrates (Fig. 3) were computed and compared to the simulations. This process was iterative until comparable results were obtained (e.g., Fig. 4). Subsequently, all computations were conducted for the other simulated structure and results presented in Table 1.

3 Results and Discussions

The results of the fractal analyses of the simulated AFM surfaces of thin films are presented in Table 1. A short description of the results in Table 1 is as follows:

- Minkowski connectivity (X): Negative values dominate the X for columnar, ballistic, and fibrous structures whereas positive dominates for pile-up particles. The profiles vary with the type of structures.
- Minkowski boundary: There are significant differences; while columnar and ballistic tend to nearly Gaussian profiles, the maximum values of boundary lengths for fibrous, and pile-up are skewed right and left, respectively.
- Minkowski volume: The profiles for columnar, ballistic and pile-up particles are symmetrical about $V = 0.5$, and exhibit S-shape [11, 20, 23]. The fibrous structures are asymmetrical and exhibit quarter-circle shaped Minkowski volume.
- Power spectral density: For columnar surface structures, the profile has a flat region at low frequencies and linearly decreasing PSD at high frequency with

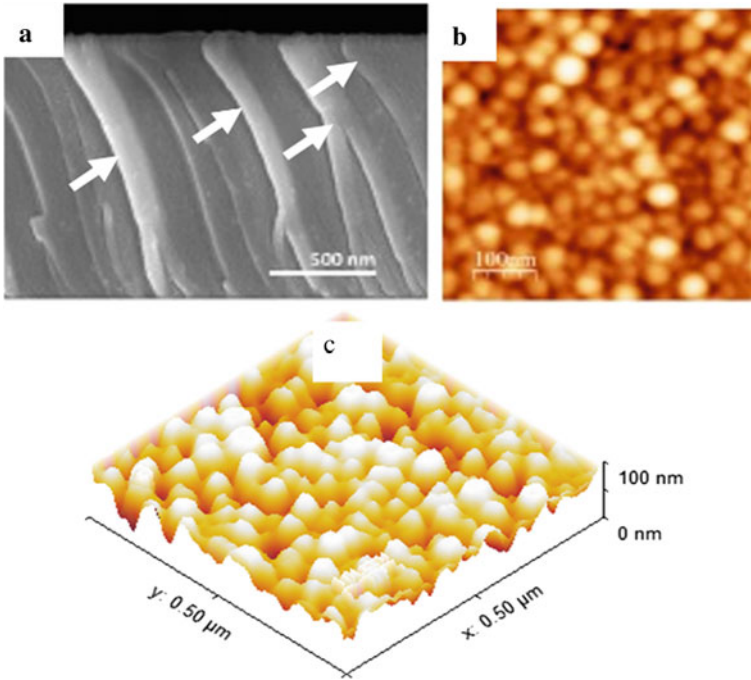


Fig. 3 **a** SEM micrograph along the cross-section of CdTe thin films deposited by RF magnetron sputtering. The white arrows show columnar structures of the films perpendicular to the substrate. **b** Showing the AFM image (scan area of $0.5 \times 0.5 \mu\text{m}^2$) at the top surface of the films. Recalibrated 3D AFM image of the CdTe films. Obtained from Camacho-Espinosa et al. [22] under open access creative commons

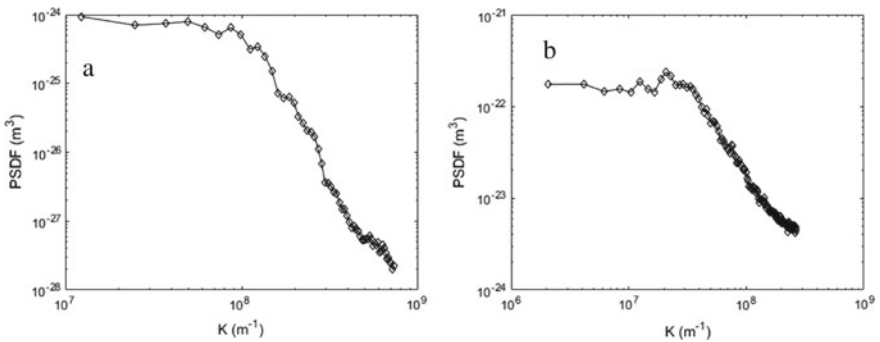


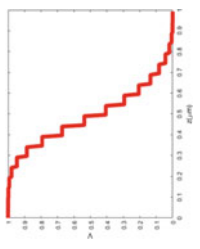
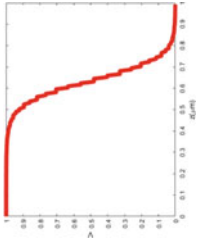
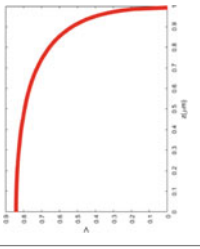
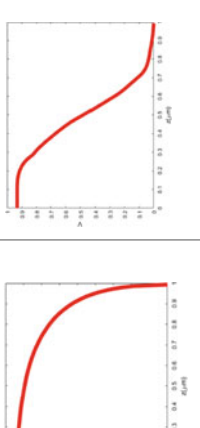
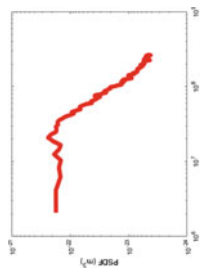
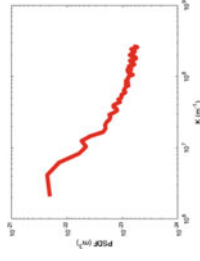
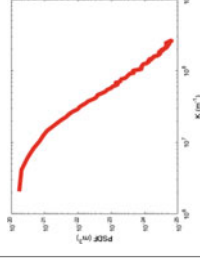
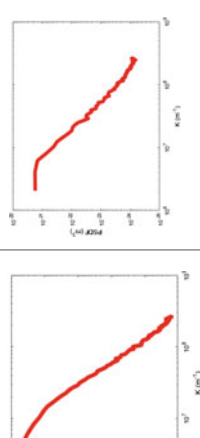
Fig. 4 Bi-logarithmic plots for power spectral density (PSDF) against the spatial frequency (k) of **(a)** typical columnar CdTe films deposited on glass substrates and **b** the corresponding simulated profile plot. The shapes of the profiles are comparable and are characterized by withers at the transition region between the flat and the linear areas of the PSDF profile

Table 1 Illustrating various fractal analyses results from different simulated (synthetic) structures of thin films

Type of structure for thin films		Type of structure for thin films		
Analysis	Columnar	Ballistic	Fibrous	Pile-up particles
Minkowski connectivity				
Minkowski boundary				

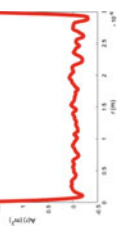
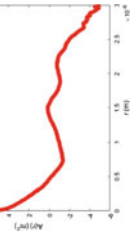
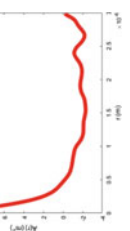
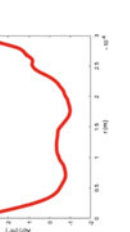
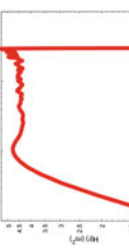




(continued)

Table 1 (continued)

Analysis	Type of structure for thin films			
	Columnar	Ballistic	Fibrous	Pile-up particles
Minkowski volume				
Power spectral density function				

(continued)

Table 1 (continued)

Analysis		Type of structure for thin films			
		Columnar	Ballistic	Fibrous	Pile-up particles
Areal autocorrelation function					
					
Height-height correlation/structure function					

withers at the transition point [21, 24, 25]. For ballistic surfaces, the 1-d PSD profile consists of flat region and nonlinearly decreasing PSD. The flat region is not clear in fibrous surfaces whereas the pile-up surfaces have distinct flat and linear regions at low and high spatial frequencies respectively.

- Areal autocorrelation (ACF): For columnar surfaces, the profile exhibit oscillatory behavior with decreasing and increasing values at low and high shifts respectively. The ACF decreases sharply to nearly $r = 1.0$ and then nearly remains constant for ballistic and fibrous. For pile-up surfaces, the ACF profile exhibit *U*-shape.
- Height-height correlation (HCF): The HCF increases with r for all surfaces up to certain values. At very large r (mounded surface characteristics) oscillatory behavior of the profile was observed for columnar and ballistic surface structures [12, 23, 25]. The flat region (at large r) is not distinct for ballistic surfaces. The HCF decreases at nearly constant r at the end of the flat region for columnar and pile-up surfaces.

4 Conclusion

The profile plots of the most common fractal analyses of thin film surfaces of different synthetic morphologies have been presented. The surfaces were generated using Gwydion software and a typical validation of the columnar structure showed that the software provides a good approximation of deposited films. Profiles of Minkowski functionals, autocorrelation, height-height correlation and power spectral density functions of the synthetic morphologies (columnar, ballistic, fibrous and pile-up particles) presented in Table 1 will be a useful reference in relating the fractal results to the films' deposition techniques and conditions.

References

1. Mwema FM, Oladijo OP, Akinlabi SA, Akinlabi ET (2018) Properties of physically deposited thin aluminium film coatings: a review. *J Alloy Compd* 747:306–323. <https://doi.org/10.1016/j.jallcom.2018.03.006>
2. Eaton P, West P (2010) *Atomic force microscopy*. Oxford University Press Inc., New York
3. Mwema FM, Akinlabi ET, Oladijo OP (2019) Correction of artifacts and optimization of atomic force microscopy imaging: a case of thin aluminum films for prosthetic applications. In: Kumar K, Paulo Davim J (eds) *Design, development, and optimization of bio-mechatronic engineering products*, IGI Global, pp 158–179. <https://doi.org/10.4018/978-1-5225-8235-9.ch007>
4. Kwoka M, Ottaviano L, Szuber J (2007) AFM study of the surface morphology of L-CVD SnO₂ thin films. *Thin solid films* 515:8328–8331. <https://doi.org/10.1016/j.tsf.2007.03.035>
5. Sobola D, Țălu S, Solaymani S, Grmela L (2017) Influence of scanning rate on quality of AFM image: study of surface statistical metrics. *Microsc Res Tech* 80(12):1328–1336. <https://doi.org/10.1002/jemt.22945>

6. Erinosh MF, Akinlabi ET, Johnson OT (2018) Characterization of surface roughness of laser deposited titanium alloy and copper using AFM. *Appl Surf Sci* 435:393–397. <https://doi.org/10.1016/j.apsusc.2017.11.131>
7. Mwema FM, Oladijo OP, Sathiaraj TS, Akinlabi ET (2018) Atomic force microscopy analysis of surface topography of pure thin aluminium films. *Mater Res Express* 5(4):1–15. <https://doi.org/10.1088/2053-1591/aabe1b>
8. Stach S, Sapota W, Țălu S, Ahmadpourian A, Luna C, Ghobadi N, Arman A, Ganji A (2017) 3-D surface stereometry studies of sputtered TiN thin films obtained at different substrate temperatures. *J Mater Sci Mater Electron* 28(2):2113–2122. <https://doi.org/10.1007/s10854-016-5774-9>
9. Țălu S, Stach S, Raoufi D, Hosseinpanahi F (2015) Film thickness effect on fractality of tin-doped In₂O₃ thin films. *Electron Mater Lett* 11(5):749–757. <https://doi.org/10.1007/s13391-015-4280-1>
10. Țălu S, Bramowicz M, Kulesza S, Solaymani S (2018) Topographic characterization of thin film field-effect transistors of 2,6-diphenyl anthracene (DPA) by fractal and AFM analysis. *Mater Sci Semicond Process* 79:144–152. <https://doi.org/10.1016/j.mssp.2018.02.008>
11. Salerno M, Banzato M (2005) Minkowski measures for image analysis in scanning probe microscopy. *Microsc Anal* 19(4):13–15
12. Yadav RP, Kumar M, Mittal AK, Dwivedi S, Pandey AC (2014) On the scaling law analysis of nanodimensional LiF thin film surfaces. *Mater Lett* 126:123–125. <https://doi.org/10.1016/j.matlet.2014.04.046>
13. Yadav RP, Dwivedi S, Mittal AK, Kumar M, Pandey AC (2012) Fractal and multifractal analysis of LiF thin film surface. *Appl Surf Sci* 261:547–553. <https://doi.org/10.1016/j.apsusc.2012.08.053>
14. Senthilkumar M, Sahoo NK, Thakur S, Tokas RB (2005) Characterization of microroughness parameters in gadolinium oxide thin films: A study based on extended power spectral density analyses. *Appl Surf Sci* 252(5):1608–1619. <https://doi.org/10.1016/j.apsusc.2005.02.122>
15. Dallaeva D, Talu S, Stach S, Skarvada P, Tomanek P, Grmela L (2014) AFM imaging and fractal analysis of surface roughness of AlN epilayers on sapphire substrates. *Appl Surf Sci* 312:81–86. <https://doi.org/10.1016/j.apsusc.2014.05.086>
16. Starodubtseva MN, Starodubtsev IE, Starodubtsev EG (2017) Novel fractal characteristic of atomic force microscopy images. *Micron* 96:96–102. <https://doi.org/10.1016/j.micron.2017.02.009>
17. Raoufi D (2010) Fractal analyses of ITO thin films: a study based on power spectral density. *Phys B Condens Matter* 405(1):451–455. <https://doi.org/10.1016/j.physb.2009.09.005>
18. Nečas D, Klapetek P (2012) Gwyddion: an open-source software for SPM data analysis. *Cent Eur J Phys* 10(1):181–188. <https://doi.org/10.2478/s11534-011-0096-2>
19. Klapetek P, Necas D, Anderson C (2013) Gwyddion user guide 1–122. <http://gwyddion.net/download/user-guide/gwyddion-user-guide-en.pdf>
20. Mwema FM, Akinlabi ET, Oladijo OP, Majumdar JD (2019) Effect of varying low substrate temperature on sputtered aluminium films. *Mater Res Express* 6(5):056404. <https://doi.org/10.1088/2053-1591/ab014a>
21. Mwema FM, Oladijo OP, Akinlabi ET (2018) Effect of substrate temperature on aluminium thin films prepared by RF-magnetron sputtering. *Mater Today Proc* 5(9/3):20464–20473. <https://doi.org/10.1016/j.matpr.2018.06.423>
22. Camach-Espinosa E, Rosendo E, Díaz T, Oliva I, Rejon V, Peria J (2014) Effects of temperature and deposition time on the RF- sputtered CdTe films preparation. *Superf. y vacío* 27(1):15–19. <http://smctsm.org.mx/ojs/index.php/SyV/article/view/148>
23. Mwema FM, Akinlabi ET, Oladijo OP (2019) Fractal analysis of hillocks: a case of RF sputtered aluminium thin films. *Appl Surf Sci* 489:614–623. <https://doi.org/10.1016/J.APSUSC.2019.05.340>
24. Shakoury R, Rezaee S, Mwema FM, Luna C, Ghosh K, Jurečka S, Țălu S, Arman A, Korpi AG (2020) Multifractal and optical bandgap characterization of Ta₂O₅ thin films deposited by electron gun method. *Opt Quantum Electron* 52(2). <https://doi.org/10.1007/S11082-019-2173-5>

25. Mwema FM, Akinlabi ET, Oladijo OP (2020) Fractal analysis of thin films surfaces: a brief overview. In: Awang M, Emamian S, Yusof F (eds) *Advances in material sciences and engineering. Lecture notes in mechanical engineering*. Springer, Singapore. https://doi.org/10.1007/978-981-13-8297-0_28